

Exciton binding energies in shallow GaAs-Al_yGa_{1-y}As quantum wells

P. E. Simmonds,* M. J. Birkett, M. S. Skolnick, W. I. E. Tagg, and P. Sobkowicz†
Department of Physics, University of Sheffield, Sheffield S3 7RH, United Kingdom

G. W. Smith
Defence Research Agency, St. Andrews Road, Malvern, Worcs WR14 3PS, United Kingdom

D. M. Whittaker
Department of Physics, University of Sheffield, Sheffield S3 7RH, United Kingdom

(Received 8 June 1994)

Strong enhancements of the exciton binding energy (E_x), compared to bulk GaAs, are deduced from high-resolution spectroscopic studies of shallow GaAs-Al_yGa_{1-y}As quantum wells, with aluminum concentrations of (1–4.5%). A clear increasing trend in E_x from 5.9 meV at 1% aluminum to 7.0 meV at 4.5% is deduced, in good agreement with the predictions of variational calculations. Even at 1%, the value of E_x represents an enhancement of 40% over that in three-dimensional GaAs. The similarity of all the spectra supports strongly the marked two dimensionality of the lowest exciton states, even for very low barrier heights.

Shallow quantum wells (QW's) are of considerable interest at the present time both from the fundamental point of view and for their potential device applications.^{1–4} In the present paper a very-high-resolution spectroscopic study of a series of shallow GaAs-Al_yGa_{1-y}As multiple QW structures with $y = 0.045, 0.02,$ and $0.01,$ respectively, is reported. Very marked enhancements of exciton binding energy (E_x) are deduced compared to bulk GaAs for conduction- and valence-band barrier heights as small as 9 and 5 meV, respectively, in the 1% Al sample. Thus, even in very shallow QW's the effects of the QW confinement potential, and hence of two dimensionality, on the exciton properties are very marked. These results are consistent with the observations of Goossen and co-workers^{1,3} of room-temperature exciton peaks and clear quantum confined Stark effects, both signatures of quasi-two-dimensionality, in structures of similar, low Al content. The presence of clear exciton peaks at 300 K allows the application of such structures as optical modulators, with the advantage that carrier sweep-out times are very short, relative to conventional high Al barrier structures.

A clear increasing trend of E_x from 5.9 meV at 1% to 7.0 meV at 4.5% is deduced from the present spectroscopic studies. The trend is found to be in good agreement with the results of variational calculations for E_x . The spectroscopic determinations of E_x are obtained from observations of 1s-2s exciton energy separations together with a small correction for the 2s binding energy.⁵ The identification of the very-well-resolved 2s exciton states is placed on a firm footing by low-field magneto-optical studies.

The experiments were carried out at 4.2 K on a series of GaAs-Al_yGa_{1-y}As structures grown by molecular-beam epitaxy at 610 °C. The structures consist of 25 repeats of 200-Å-thick GaAs QW's and 500-Å Al_yGa_{1-y}As barriers with $y = 0.01, 0.02,$ or $0.045.$ A 1000-Å-thick Al_{0.02}Ga_{0.98}As layer was also grown for comparison with the $y = 0.02$ multiple QW sample. The Al compositions (y) were determined during growth from $y = R_{\text{AlAs}} / (R_{\text{GaAs}} + R_{\text{AlAs}}),$ where R_{GaAs} and

R_{AlAs} are GaAs and AlAs growth rates, respectively, measured by reflection high-energy electron-diffraction oscillation techniques to an accuracy better than 1%.⁶ The expression for y will hold when there is no preferential loss of either group-III species, as is the case for Al_yGa_{1-y}As growth below 640 °C. The reliability of the Al composition is demonstrated by the observations of features in the QW spectra arising from transitions at energies close to those of the expected Al_yGa_{1-y}As band-gap energies. Photoluminescence (PL) and PL excitation (PLE) spectra were excited with 0.1 W/cm² of light from an Ar-laser pumped Ti-sapphire laser. PL was dispersed by a 0.85-m double spectrometer and detected with a cooled GaAs photomultiplier. Magnetic-field spectra were obtained in a vertical bore superconducting magnet.

PL and PLE spectra for the 4.5% sample are shown in Figs. 1(a) and 1(b), respectively. The very small Stokes shift (0.1 meV) and the narrow linewidths (0.6 meV) demonstrate the high sample quality. The transitions are identified by comparison with the results of three-band $\mathbf{k} \cdot \mathbf{p}$ calculations,⁷ from the low magnetic-field dependence of the PLE spectra discussed below (shown in the inset for the 1523–1533-meV region), and from circular polarization experiments to distinguish heavy- and light-hole features. The first two PLE peaks arise from 1s exciton, $n = 1$ heavy-hole (HH) and $n = 1$ light-hole transitions to the $n = 1$ electron subband (E_{11h} and E_{11l} , respectively). To higher energy, E_{12h} , $E_{11h}(2s)$, and $E_{11l}(2s)$ exciton transitions are observed. Parity forbidden E_{12h} transitions are seen in all the samples investigated, probably due to the presence of weak electric fields (3–5 kV/cm) arising from surface Fermi-level pinning.^{10–12} To higher energy, the most prominent features arise from E_{13h} , E_{22h} , and transitions at the Al_yGa_{1-y}As barrier exciton-gap energy [$E_{gx}(\text{barr})$], as marked on Fig. 1. E_{13h} has the characteristic Fano-resonance line shape of a sharp transition coupled to a lower energy continuum.^{13,10}

The E_{11h} and E_{11l} transition energies and the $E_{1s-2s}(h), E_{1s-2s}(l)$ energy separations are summarized in Table I.

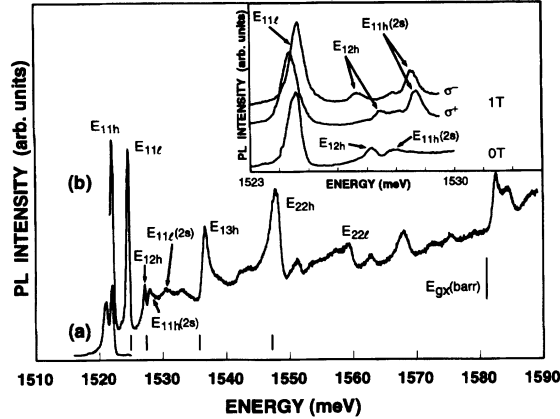


FIG. 1. Photoluminescence (PL) and PL excitation (PLE) spectra for sample with 4.5% Al barriers in (a) and (b), respectively. The weaker lower-energy peak in the PL spectrum is defect related. The vertical lines below the PLE spectra are calculated transition energies for E_{11l} , E_{12h} , E_{13h} , and E_{22h} , respectively. E_{gx} (barr) indicates the $Al_yGa_{1-y}As$ barrier exciton energy for the $Al_yGa_{1-y}As$ band-gap variation of 14.8y meV measured for the 2% Al sample. The inset shows expanded spectra at $B=0$ and 1 T (σ^+ , σ^- polarization).

Knowledge of these separations permits a spectroscopic determination of the exciton binding energies (E_x), once a small correction for the $2s$ exciton binding energy is made, since $E_x = E_{1s-2s} + E_x(2s)$. Exciton binding-energy calculations we have carried out, described later, give $E_x(2s) = 1.1$ meV, and so E_{xh} and E_{xl} are deduced to be $5.9 + 1.1 = 7.0 (\pm 0.1)$ and $5.8 + 1.1 = 6.9 (\pm 0.1)$ meV, respectively. These values constitute an enhancement of 65% over the exciton binding energy of 4.2 meV in bulk, three-dimensional (3D) GaAs,¹⁴ and demonstrate clearly the significant two dimensionality of the exciton states in QW's with 4.5% Al barriers. The vertical lines below the principal peaks are calculated transition energies using the three-band $\mathbf{k} \cdot \mathbf{p}$ model, with a constant exciton binding energy of 7 meV assumed for all transitions. The calculated energies are shifted up slightly (by 0.5 meV) to bring the predicted E_{11h} lines into agreement with experiment. In all cases the agreement is good, to within 1 meV, thus substantiating the assignments of the higher energy transitions of Fig. 1.

PL and PLE spectra for the 2% and 1% samples are pre-

TABLE I. Transition energies and exciton binding energies (meV).

	4.5%	2%	1%
E_{11h}	1521.85	1519.85	1518.44
E_{11l}	1524.45	1521.75	1519.75
$E_{1s-2s}(h)$	5.9	5.3	4.8
$E_{1s-2s}(l)$	5.8	5.2	4.7
$E_{xh} = E_{1s-2s}(h) + E_{xh}(2s)$	7.0	6.4	5.9
$E_{xl} = E_{1s-2s}(l) + E_{xh}(2s)$	6.9	6.3	5.8
$E_{xh}(1s)$ (theory)	6.1	5.7	5.4
$E_{xh}(2s)$ (theory)	1.1	1.07	1.05
E_{11h}^{cont} (calc)	1528.34	1526.26	1524.47
E_{xh} (abs)	6.5	6.4	6.0

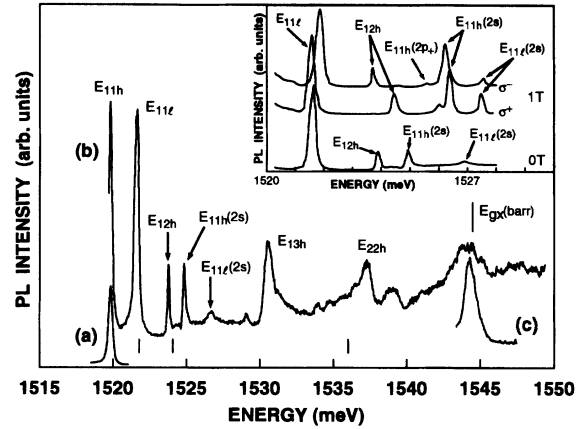


FIG. 2. (a) and (b) As in Figs. 1(a) and 1(b) but for the 2% Al barrier sample. The vertical lines indicate calculated transition energies for E_{11l} , E_{12h} , and E_{22h} . (c) is the PLE spectrum for a 1000-Å-thick layer of $Al_{0.02}Ga_{0.98}As$. Inset: as in Fig. 1 inset but for the 2% Al sample.

sented in Figs. 2(a) and 2(b), and 3(a) and 3(b), respectively. Once again very-high-quality spectra are seen, with Stokes shift < 0.1 meV and very narrow linewidths (0.13 meV for the 1% sample) being observed. The overall appearance of the spectra with E_{11h} , E_{11l} , E_{12h} , $E_{11h}(2s)$, $E_{11l}(2s)$, and E_{13h} transitions in the low-energy region of the PLE is very similar to that for the 4.5% sample in Fig. 1. The similarity of the spectra indicates strongly that even in samples with 1% barriers (total band-gap discontinuity 15 meV) the effects of two dimensionality are very marked.¹⁵

Increasing quenching of below barrier QW continuum transitions relative to the exciton transitions is observed in the sequence 4.5% to 2% to 1% between Figs. 1(b), 2(b), and 3(b). This phenomenon increases the prominence of weak excited-state transitions in the spectra. It arises since with reducing barrier height the probability of migration of carriers created with finite kinetic energy to nonradiative centers at either the substrate or surface becomes increasingly great. Similar quenching of continuum transitions has been reported for short-period superlattices.^{16,17}

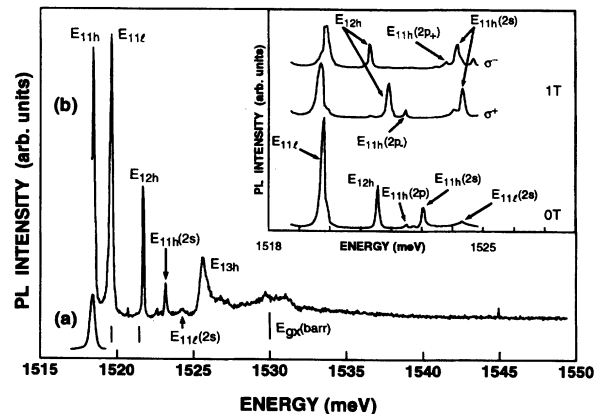


FIG. 3. (a) and (b) As in Figs. 1(a) and 1(b) but for the 1% Al sample. The vertical lines indicate calculated E_{11l} , E_{12h} energies. Inset: as in Fig. 1 but for the 1% Al sample.

The PLE spectrum of a 1000-Å-thick $\text{Al}_y\text{Ga}_{1-y}\text{As}$ layer with aluminum composition $y=0.02$, is shown in Fig. 2(c). The PLE peak arises from free exciton transitions in $\text{Al}_{0.02}\text{Ga}_{0.98}\text{As}$. The exciton feature in Fig. 2(c) agrees well in energy with the feature identified as arising from $\text{Al}_y\text{Ga}_{1-y}\text{As}$ barrier transitions for the QW sample in Fig. 2(b). The $\text{Al}_y\text{Ga}_{1-y}\text{As}$ barrier energies marked on Figs. 1 and 3 are calculated using an $\text{Al}_y\text{Ga}_{1-y}\text{As}$ band-gap variation of 14.8y meV deduced from Fig. 2(c),¹⁸ and are seen to agree well in all cases with peaks identified as $\text{Al}_y\text{Ga}_{1-y}\text{As}$ barrier transitions.

The energies of the 1s and 2s E_{11h} and E_{11l} exciton transitions for the 2% and 1% samples are tabulated in Table I. Exciton binding energies are again deduced from the 1s-2s energy separations, plus the calculated values of 1.07 and 1.05 meV for the 2s binding energies for the 2% and 1% samples. Values of $E_{xh}=6.4$ meV at 2% and 5.9 meV at 1% are deduced (and E_{xl} values of 6.3 and 5.8 meV, respectively). Thus, a clear decreasing trend of exciton binding energy from 7.0 meV at 4.5% down to 5.9 meV at 1% is found from these spectroscopic studies.

Exciton binding energies were calculated using variational techniques with a nonseparable wave function of the form $\varphi_e(z_e)\varphi_h(z_h)\exp[-\sqrt{r^2+(z_e-z_h)^2}/\lambda]$, where $\varphi_i(z_i)$ are QW envelope functions for electrons and holes. Decoupled heavy- and light-hole bands were assumed. Such a wave function, nonseparable into in-plane and perpendicular terms, is expected to be appropriate for shallow QW's where the Coulomb interaction is of the same order as the QW confinement potential.¹⁹ Values of E_{xh} of 6.1, 5.7, and 5.4 meV were obtained from the calculations [$E_{xh}(1s)$ (theory) in Table I] for the 4.5%, 2%, and 1% samples, respectively. The overall trend of E_{xh} with decreasing Al from the experiments (7 to 6.4 to 5.9 meV) is found to be reproduced well, although in all cases the theoretical values are too low (by 0.5–0.9 meV), possibly because of the neglect of heavy-hole–light-hole mixing in the calculations.

The strong enhancements of exciton binding energy can be understood from examination of the electron and hole wave functions. For the 4.5% Al QW the probability of finding an $E1$ electron in the well is 95% and for an HH1 hole is 97%. Even for the 1% sample, the confinement of $E1$ electrons and HH1 holes in the well is marked, with probabilities of 75% and 86%, respectively, being calculated. Since the QW's are of width 200 Å, of order of the 3D exciton Bohr radius, a significant increase of exciton binding energy relative to three dimensions is expected, as calculated, and observed in the experimental studies.

A key point in the deduction of E_x from the experimental data is the correct identification of the 2s transitions, particularly since they arise close in energy to the sharp, normally forbidden, E_{12h} peaks. The detailed magnetic-field experiments substantiate these assignments very clearly. Spectra at $B=0$, and at 1 T for σ^+ and σ^- polarizations, are shown in the insets to Figs. 1, 2, and 3, and a fan diagram of transition energies against magnetic field for the most prominent tran-

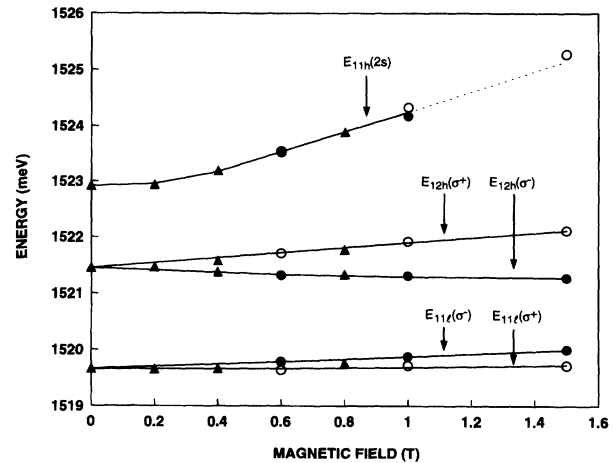


FIG. 4. E_{11l} , E_{12h} , and $E_{11h}(2s)$ transition energies as a function of magnetic field up to 1.5 T for the 1% Al sample of Fig. 3. Triangles, unpolarized spectra; open circles, σ^+ polarization; filled circles, σ^- polarization. The full lines are guides to the eye.

sitions for the 1% sample is shown in Fig. 4. In all cases the peak labeled 2s shows a strong upshift in energy, whereas the peak labeled E_{12h} splits into two with only small displacement of its center of gravity to higher energy up to 1.5 T. The E_{12h} splitting is several times larger than that observed for E_{11h} , E_{11l} , or $E_{11h}(2s)$ transitions, with the σ^- (σ^+) component lower (higher) in energy. This behavior is characteristic of $E_{11h}(2s)$ and E_{12h} peaks, respectively,¹⁰ and confirms the proposed identifications.²⁰ Very similar results for these two transitions were obtained by Vina *et al.* and Iimura *et al.* in magnetic-field studies of highly resolved spectra for QW's with high Al content in the barriers.^{10,11}

The deduction of the exciton binding energies by the above spectroscopic technique based on the energy separation of very sharp spectral lines is thus placed on a very firm basis. Values for E_x can also be deduced from the absolute energies of the E_{11h} exciton transitions by comparison with calculated $n=1$ heavy hole and $n=1$ electron subband free particle, continuum transition energies [$E_{11h}^{\text{cont}}(\text{calc})$ in Table I].²¹ The energy separation between $E_{11h}^{\text{cont}}(\text{calc})$ and E_{11h} is equal to E_{xh} . Values of E_{xh} [$E_{xh}(\text{abs})$ in Table I] of 6.5, 6.4, and 6.0 meV are obtained in this way, again reproducing the trend of E_{xh} deduced from the 1s-2s separations, and in quantitative agreement within experimental error with the accurate values deduced from $E_{1s-2s}(h) + E_{xh}(2s)$.²²

In conclusion, a very-high-resolution spectroscopic study of a series of GaAs- $\text{Al}_y\text{Ga}_{1-y}\text{As}$ QW's has been reported. Marked enhancements of exciton binding energy have been deduced, even for the very low values of barrier height studied. The strong similarity of all the spectra supports the deduction of marked two dimensionality of the lowest exciton states, even for barriers containing only 1% aluminum. The trend of increasing E_x with Al composition has been shown to be in good agreement with the predictions of variational calculations.

*Permanent address: Department of Physics, University of Wollongong, Wollongong, NSW 2500, Australia.

†Permanent address: Institute of Physics of the Polish Academy of

Sciences, Al Lotnikow 32/46, 02 668, Warsaw, Poland.

¹K. W. Goossen, J. E. Cunningham, and W. Y. Jan, *Appl. Phys. Lett.* **57**, 2582 (1990).

- ²J. Feldmann, K. W. Goossen, D. A. B. Miller, A. M. Fox, J. E. Cunningham, and W. Y. Jan, *Appl. Phys. Lett.* **59**, 66 (1991).
- ³K. W. Goossen, J. E. Cunningham, M. D. Williams, F. G. Storz, and W. Y. Jan, *Phys. Rev. B* **45**, 13 773 (1992).
- ⁴I. Brener, W. H. Knox, K. W. Goossen, and J. E. Cunningham, *Phys. Rev. Lett.* **70**, 319 (1993).
- ⁵See, e.g., P. Dawson, K. J. Moore, G. Duggan, H. I. Ralph, and C. T. Foxon, *Phys. Rev. B* **34**, 6007 (1986).
- ⁶J. H. Neave, B. A. Joyce, P. J. Dobson, and N. Norton, *Appl. Phys. A* **31**, 1 (1983).
- ⁷The input parameters in the $\mathbf{k}\cdot\mathbf{p}$ model were $m_{\text{HH}}=0.34m_0$, spin-orbit splitting $\Delta_{\text{so}}=340$ meV, $\mathbf{k}\cdot\mathbf{p}$ momentum matrix element 24 326 meV (the same values of m_{HH} , Δ_{so} , and $E_{\mathbf{k}\cdot\mathbf{p}}$ were used for the wells and barriers), $E_g(\text{GaAs})=1519.2$ meV, $E_g(\text{Al}_y\text{Ga}_{1-y}\text{As})=1519.2+14.2$ meV, and conduction- and valence-band offsets of 9.2y and 5.0y meV, corresponding to a conduction- and valence-band offset ratio of 65:35. The $\text{Al}_y\text{Ga}_{1-y}\text{As}$ E_g variation with y is an average of the value of 13.6y meV of Ref. 8 and the value of 14.8y meV deduced here. The 65:35 offset ratio is that employed in Ref. 9.
- ⁸C. Bosio, J. L. Staehli, M. Gazzi, G. Burri, and R. A. Logan, *Phys. Rev. B* **38**, 3263 (1988).
- ⁹J. W. Orton, P. P. Fewster, J. P. Gowers, P. Dawson, K. J. Moore, P. J. Dobson, C. J. Curling, C. T. Foxon, K. Woodbridge, G. Duggan, and H. I. Ralph, *Semicond. Sci. Technol.* **2**, 597 (1987).
- ¹⁰L. Vina, G. E. W. Bauer, M. Potemski, J. C. Maan, E. E. Mendez, and W. I. Wang, *Phys. Rev. B* **41**, 10 767 (1990).
- ¹¹Y. Iimura, Y. Segawa, G. E. W. Bauer, M. M. Lin, Y. Aoyagi, and S. Namba, *Phys. Rev. B* **42**, 1478 (1990).
- ¹²L. C. Andreani and A. Pasquarello, *Europhys. Lett.* **6**, 259 (1988).
- ¹³D. Y. Oberli, G. Böhm, G. Weimann, and J. A. Brum, *Phys. Rev. B* **49**, 5757 (1994).
- ¹⁴D. D. Sell, *Phys. Rev. B* **6**, 3750 (1972).
- ¹⁵For the 2% and 1% samples, the assignment of E_{13h} is suggested by the similarity with the corresponding 4.5% spectra. At 2% and 1%, a confined $n=3$ hole subband is not expected. However, excitons with reduced E_x are likely to be formed from the lowest-energy extended hole states.
- ¹⁶A. Chomette, B. Lambert, B. Clerjaud, F. Clerot, H. W. Liu, and A. Regreny, *Semicond. Sci. Technol.* **3**, 351 (1988).
- ¹⁷K. J. Moore, G. Duggan, P. Dawson, C. T. Foxon, N. J. Pulsford, and R. J. Nicholas, *Phys. Rev. B* **39**, 1219 (1989).
- ¹⁸The free exciton peak in Fig. 2(c) for $\text{Al}_{0.02}\text{Ga}_{0.98}\text{As}$ arises at 1544.5 meV. Taking the free exciton gap in GaAs as 1515.0 meV from Ref. 14, and assuming negligible change in E_{gx} between GaAs and $\text{Al}_{0.02}\text{Ga}_{0.98}\text{As}$, a band-gap discontinuity of 14.8y meV between $\text{Al}_y\text{Ga}_{1-y}\text{As}$ and GaAs (1544.5 - 1515.0)/2=14.8 meV is deduced. This value is in very reasonable agreement with the value of 13.6 meV for 0.1 < y < 0.75 of Ref. 8.
- ¹⁹G. Bastard, E. E. Mendez, L. L. Chang, and L. Esaki, *Phys. Rev. B* **26**, 1974 (1982).
- ²⁰Weak additional structure observed between E_{12h} and $E_{11h}(2s)$, most clearly seen for the 1% samples in the Fig. 3 inset near 1523 meV, can probably be attributed to $E_{11h}(2p)$. In magnetic field, the weak but clearly resolved peaks labeled $E_{11h}(2p_{\pm})$ in Figs. 2 and 3 (insets) originate from this energy region, and exhibit polarization similar to that described for $E_{11h}(2p_{\pm})$ in Ref. 10.
- ²¹The parameters given in Ref. 7 were used to obtain the $E_{11h}^{\text{cont}}(\text{calc})$ values given in Table I.
- ²²The values of $E_{xh}(\text{abs})$ are subject to errors of ± 0.1 meV from the measured spread of E_{11h} values across the center 2 cm of the wafer, ± 0.2 meV in $E_{11h}^{\text{cont}}(\text{calc})$ from 5% uncertainty in the Al compositions, and ± 0.2 meV in $E_{11h}^{\text{cont}}(\text{calc})$ from 10% uncertainty in the offset values. The final source of error is systematic and does not affect the comparison between respective $E_{xh}(\text{abs})$ values for the different samples. Thus the deduced trend of $E_{xh}(\text{abs})$ values is at the limits of the errors (± 0.3 meV), whereas the individual values are subject to larger values of ± 0.5 meV.